Nonlinear Registration Based on the Approximation of Radial Basis Function Coefficients

Jia-Xiu Liu[1] Yong-Sheng Chen[1] Li-Fen Chen[2,3,*]

[1]Department of Computer Science, National Chiao Tung University, Hsinchu 300, Taiwan, ROC
[2]Institute of Brain Science, National Yang-Ming University, Taipei 112, Taiwan, ROC
[3]Department of Medical Research and Education, Taipei Veterans General Hospital, Taipei 112, Taiwan, ROC

Received 21 Jul 2008; Accepted 19 Aug 2008

Abstract

Nonlinear registration is a technique which can accommodate the deformation of structures. It is widely applied to many applications of medical images, such as the analysis of disease characterization and the observation of brain degeneration. This paper presents an efficient approach which can accurately register images. Hierarchical regular meshes of Wendland's radial basis functions are adopted to model the deformation of images from coarse to fine. To efficiently establish the spatial relationship between images, an approximation method is proposed to determine the coefficients of basis functions according to the spatial interpretation in deformation. This results an image registration accomplished by a series of fast optimizations with only three degrees of freedom, and avoids the difficulties of direct searching for all coefficients in a huge optimization space. Experimental results indicate that the proposed method is much more accurate than statistical parametric mapping 2 (SPM2) and is superior to hierarchical attribute matching mechanism for elastic registration (HAMMER) and automatic registration toolbox (ART) in both accuracy and efficiency.

Keywords: Nonlinear registration, Radial basis function (RBF), Magnetic resonance imaging (MRI)

1. Introduction

Registration is an important step in many applications of medical images. For example, the fusion of positron emission tomography (PET) and magnetic resonance (MR) images gives the opportunity to delineate anatomical and functional information at the same time. The registration results of images acquired at different times can be used to observe temporal changes. Moreover, the average of brain images which are normalized to the Talairach space gives the prior knowledge of the human brain and it also acts a bridge to Brodmann's map.

A typical registration method needs a transformation function to describe the spatial mapping between images. Rigid or affine transformation is appropriate for many applications, such as the alignment of brain images scanned from the same subject because we can assume the motion is constrained by the skull. Extending the polynomial orders of affine transformation can form a more complicated registration model [1]. All these methods can only cope with global differences between images. For many applications, however, more sophisticated approaches are required to eliminate the anatomical variation across subjects, such as the structural analysis of brains.

In this work, we apply radial basis functions (RBFs) to develop an accurate and efficient nonlinear registration technique. Hierarchical meshes of RBFs are used to model image deformation from coarse to fine. Although a large number of RBFs were proposed, Wendland's RBF is adopted because of the low computational complexity and the compact support property [2]. The compact support, which means that the influence of the function is constrained in a local region, is a reasonable property in deformation modeling because the registration of local structures should not affect the deformation of remote regions. According to this property, we propose an efficient method to accurately approximate the coefficients of RBFs. At present, the proposed method is applied to register MR images of human brains. Simulated MR images were constructed for the validation, and the experimental results indicate that our method is much accurate than statistical parametric mapping 2 (SPM2) [3] and is superior to hierarchical attribute matching mechanism for elastic registration (HAMMER) [4] and automatic registration toolbox (ART) [5], in terms of both efficiency and accuracy.

In this paper, nonlinear registration techniques are first reviewed according to the adopted transformation model. Then, the new registration approach and implementation issues are introduced in detail. Finally, we describe a validation procedure and show the comparison results using 58 image

* Corresponding author: Li-Fen Chen
Tel: +886-2-28267384; Fax: +886-2-28273123
E-mail: lfchen@ym.edu.tw

pairs with ground truths.

2. Review

Numerous nonlinear registration approaches were proposed in the past decades. According to the transformation models, we classify them into three main categories: elastic and fluid methods, finite element methods (FEM), and the techniques using basis functions.

Elastic methods register images based on the balance of internal and external forces, which represent the constraint of deformation smoothness and the similarity measurement between images, respectively [6]. Because of the limitation of the high internal forces, these schemes may inadequately apply to model highly localized deformation, such as the bending of cerebral cortex. To overcome this problem, the variant, fluid model, relaxes the energy constraint, but they face the risk of false registration instead [7].

A typical FEM registers images using segmented objects which are usually represented as the meshes of tetrahedrons or hexahedrons [4,8-9]. These methods can deform objects in a more realistic way because different energy terms can be assigned to objects according to the physical properties. However, two major drawbacks with this method results from the preprocessing stages. Firstly, the segmentation errors of objects always contribute to the deviations of registrations. Secondly, the computational complexity is usually high because a great deal of small elements are required to represent the segmented objects in order to achieve an accurate registration.

Linear combinations of basis functions are also widely applied to describe the spatial mapping between images. These methods can be further classified into two major categories according to the characteristics of the adopted functions.

The methods of the first class establish the spatial mapping between images using wavelets [10-11] or discrete cosine transform (DCT) [3], in which each function encodes a particular frequency of deformation in registration. A large number of basis functions are required in order to model the subtle deformation of images. This causes two problems in practical applications that the computational complexity is often high and it is usually difficult to obtain good results by the direct searching in the large optimization space.

The methods of the second class, referred as landmark-based approaches, register images under the assumption that a set of corresponding control points or landmarks are identified. Lots of landmark-based basis functions were proposed for image registrations, such as thin-plate splines (TPS) [12-13], Gaussian [14], multi-quadrics [13], inverse multi-quadrics [15], and Wendland's RBF [2]. Given a set of corresponding landmarks, these approaches can easily solve the mapping relation between images. However, the labor-intensive identifications of landmarks are not only time-consuming but always prone to errors.

Regular distribution of landmark-based basis functions can be used to avoid the manual selections of control points, and this enables an automatic registration by optimizing the coefficients of basis functions [16-17]. These approaches have the same drawbacks as those methods in the first class, and may be even worse. Especially, the number of basis functions is usually considerably large and this aggravates the situations. To improve these, Likar *et al.* divided images and applied affine registrations to the corresponding sub-regions [18]. The centers of the registered sub-regions were regarded as the corresponding control points, but this has the drawback that the determined pairs of control points do not guarantee a good spatial mapping. Rohde *et al.* repeatedly applied few RBFs to register image regions which are not well registered [19]. A problem with this method is that the supports of the RBFs of the identified regions were constrained to be non-overlapped, but this could lose chances to register the regions between the identified ones.

3. Methods

Our new nonlinear registration technique contains three main components, including 1) a transformation function T which establishes the spatial mapping between a test image, I_A, and a reference image, I_B, 2) a cost function used to measure the registration quality, and 3) the proposed method used to efficiently approximate image transformation such that the cost is minimized. Combining these, image registration is formulated as an optimization problem with the objective function:

$$\hat{T} = \arg\min_{T} Cost(I_A, I_B; T). \tag{1}$$

3.1 Image deformation modeling

The registration of two images is accomplished by the hierarchical meshes of basis functions, which are regularly distributed, and represented as the accumulation of coarse-to-fine deformation:

$$T(\mathbf{p}) = \mathbf{p} + \sum_{l=1}^{L} \mathbf{D}^l(\mathbf{p}). \tag{2}$$

The displacement function $\mathbf{D}^l$ at mesh level l contains three interpolators which are composed by the linear combinations of basis functions:

$$\mathbf{D}^l(\mathbf{p}) = (D_x^l(\mathbf{p}), D_y^l(\mathbf{p}), D_z^l(\mathbf{p})),\ l = 1, \ldots, L \tag{3}$$

$$D_i^l(\mathbf{p}) = \sum_{j=1}^{N_l} c_{ij}^l \theta_s(\left\|\mathbf{p} - \mathbf{r}_j^l\right\|),\ i = \mathrm{x}, \mathrm{y}, \mathrm{z}, \tag{4}$$

where D_x^l, D_y^l, and D_z^l represent the displacement functions in three dimensions, respectively, θ_s is the basis function with support s, $\mathbf{r}_j^l$ and c_{ij}^l are the centers and the corresponding coefficients of the basis functions, and N_l is the number of basis functions applied at mesh level l.

Wendland's RBF is adopted in this work because it can efficiently achieve accurate registration results. Letting $\theta(t) = \theta(t/s)$, the Wendland's RBF is defined as [2]:

$$\theta(t) = \begin{cases} (1-t)^4(4t+1), & 0 \le t < 1 \\ 0, & 1 \le t \end{cases}. \tag{5}$$

The induced influence is bounded by the support length

and is inversely proportional to the distance from its center, as shown in Figure 1. A compact supported basis function is more reasonable in deformation modeling because the effects of registration for local structures should not propagate to the whole image domain. This property also implies that the evaluation of the spatial mapping for each point needs only a few terms in Eq. (4), therefore, the computational complexity of image transformation can be greatly alleviated. Given 16^3 compact supported basis functions, for example, the number of the function evaluations for the transformation of each point can be dramatically reduced from 3×2^{12} to a small k, where k depends on the number of basis functions which supports to the point. Another advantage of Wendland's RBF is that the evaluation is relatively efficient in comparison with other choices, such as wavelets, B-splines, and Wu's RBF.

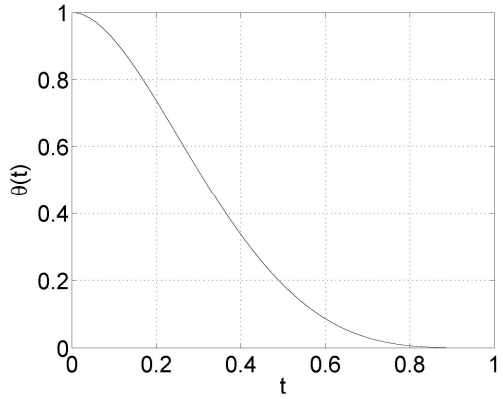

Figure 1. The induced influence of Wendland's RBF is bounded by the support and is inversely proportional to the distance from its center, t=0.

3.2 Approximation of RBF coefficients

A major drawback of the image registration accomplished by the hierarchical meshes of basis functions is the dramatic increase of the function number. This results in a difficult optimization problem because there are a lot of coefficients that must be determined to establish the spatial mapping between images. Taking a 16×16×16 mesh as an example, the direct search in the optimization space with 12,288 degrees of freedom (DOF) is not only difficult but also time-consuming.

To achieve an accurate and efficient registration, we approximate the coefficients of Wendland's RBFs in a regular mesh according to the spatial interpretations in deformation. Firstly, each mesh grid associates with the centers of three basis functions, and the influences of these functions form a specific deformation pattern. Therefore, an image registration can be regarded as the accumulation of the deformation patterns generated from the distributed mesh grids. Secondly, the influence of each basis function is constrained in a local region and rapidly decreases with the distance from its center because of the properties of Wendland's RBF. This means that the major objective of each deformation pattern is to register the supported area well, especially the region nearby the center, as shown in Figure 2.

According to the observations, the coefficients of basis functions, $\hat{C}_j^L$, associated with each mesh grid, j, are estimated by minimizing the registration cost of the image region near the center using the simplex optimization method:

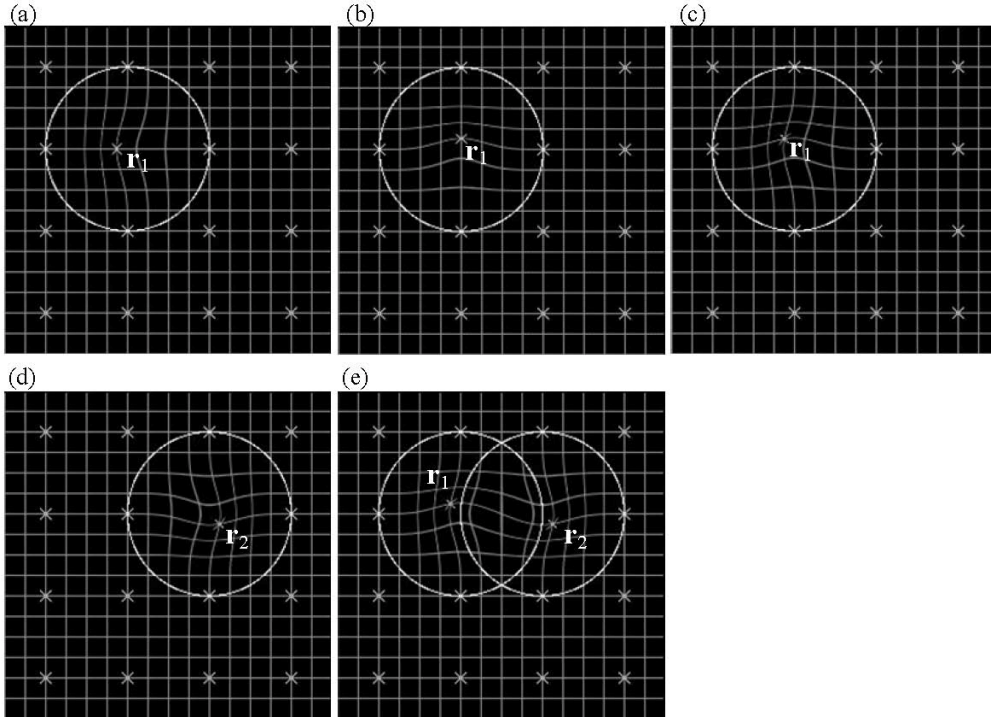

Figure 2. The deformation effects of Wendland's RBFs induced by setting the coefficients of $\mathbf{r}_1$ in x, (a), and y, (b), direction as 10 and -10, respectively. (c) Setting all the coefficients of $\mathbf{r}_1$, the induced deformation is the accumulated effects of (a) and (b). (d) The deformation induced by function $\mathbf{r}_2$. (e) Setting the coefficients for $\mathbf{r}_1$ and $\mathbf{r}_2$, the image deformation is the accumulation of the influences of all basis functions.

$$T(\mathbf{p}) = \mathbf{p} + \sum_{l=1}^{L-1} \mathbf{D}^l(\mathbf{p}) + \hat{C}_j^L \, \theta_s\left(\left\|\mathbf{p} - \mathbf{r}_j^L\right\|\right), \tag{6}$$

where $\hat{C}_j^L = \left[\hat{c}_{xj}^L \quad \hat{c}_{yj}^L \quad \hat{c}_{zj}^L\right]^T$. Therefore, an image registration using a mesh of basis functions is reduced to a series of optimization problems. The DOF of each optimization is only three, hence, the coefficients can be efficiently determined because of the small search space. Directly combining the estimated coefficients at each mesh level obtains a spatial transformation with deviations due to the overlaps between the supports of basis functions. Two strategies are applied to solve this problem and achieve accurate registration. First, instead of the whole area supported by basis functions, only the region nearby the center is used to evaluate the cost. The region is defined as the sphere with radius γs centered at the mesh grid, where s is the support length and $\gamma \in [0,1]$ defines the area used to measure the image similarity. This not only reduces the estimation error but also facilitates efficiency. Second, the approximated coefficients are weighted to form the image transformation:

$$T(\mathbf{p}) = \mathbf{p} + \sum_{l=1}^{L-1} \mathbf{D}^l(\mathbf{p}) + \beta \sum_{j=1}^{N_L} \hat{C}_j^L \, \theta_s\left(\left\|\mathbf{p} - \mathbf{r}_j^L\right\|\right), \tag{7}$$

where β is a weighting parameter.

3.3 Cost function of registration

A cost function is defined to quantify the registration quality between a reference image I_A and a test image I_B which is transformed by function T:

$$Cost(I_A, I_B; T) = -S(I_A, I_B; T) + E(T). \tag{8}$$

The first term S measures the similarity of images, and the other function, E, is a penalty term which describes the deformation energy results from T. The parameter α defines the tradeoff between the image similarity and the deformation smoothness.

The choice of a similarity measure primarily depends upon the characteristics of images in applications. The quantifications of the intensity dependence between images are applied with successes for multimodal registrations (see [20-21] for reviews). The criteria of this type, such as mutual information (MI) [22] and correlation ratio (CR) [23], are also quite adequate for unimodal registrations because they are relatively robust to the noise, the intensity contrast, and the intensity inhomogeneity of images. Both CR and MI could be applied in this work, but CR is adopted because it is superior to MI in accuracy and efficiency, as reported in [23-24]. Pluim *et al.* also indicated that different interpolation approaches can result in different artifact patterns in the optimization functions [25].

Let N be the voxel number of the overlapping region Ω between the test image I_A and reference image I_B. Considering that there are K histogram bins Y_i in I_B and each contains N_i voxels, $i = 1 \ldots K$, the formula of CR is expressed as:

$$CR = \frac{1}{\mathrm{Var}(I_A)} \sum_{i=1}^{K} \frac{N_i}{N} \mathrm{Var}(X_i), \tag{9}$$

where $\mathrm{Var}(I_A)$ is the intensity variance of the test image in Ω, X_i is the voxels of the test image which belongs to Ω and are mapped to the same histogram bin of the reference image, and $\mathrm{Var}(X_i)$ is the intensity variance of X_i. Two widely applied regularization methods are the Laplacian model and the thin-plate model. The former method is adopted because it can be efficiently evaluated:

$$E(T) = \frac{1}{V} \iiint \left[\left(\frac{\partial T}{\partial x}\right)^2 + \left(\frac{\partial T}{\partial y}\right)^2 + \left(\frac{\partial T}{\partial z}\right)^2\right] dx \, dy \, dz \tag{10}$$

where V is the volume of the estimated region.

3.4 Implementation

There are two hierarchical structures in the proposed registration method in which the data complexity and the warp complexity increase level by level. The use of image pyramids facilitates both the efficiency and the accuracy because image data can be greatly reduced and the local minima traps of optimizations can be escaped. The use of hierarchical regular meshes of Wendland's RBFs models the structure differences from coarse to fine. L meshes were applied, and $2l \times 2l \times 2l$ basis functions are regularly placed on the voxel positions of the image domain at level l, where l=1, …, L.

Another important parameter is the setting for the support length of basis functions. The support length at each mesh level is defined as k times the minimum distance between the centers of functions. From practical experience, k=1.5 can achieve balance between the efficiency and the accuracy of registration.

The computational complexity of this work is mostly determined by the evaluation of basis functions because each optimization task has to repeatedly transform numerous image voxels. The execution time of each registration task is also remarkable, though the proposed approximation method only evaluates the cost of a small image region and the transformation of each point needs only three function evaluations. Instead of all direct function evaluation, the lookup tables of Wendland's RBF are built beforehand to further improve registration efficiency.

Finally, we summarize the algorithm of the proposed nonlinear registration method in the following:

apply *affine or rigid registration*
set *the deformation modeling scale l to the coarest level 1*
while *l < the user-defined finest deformation scale L*
  downsample *images to the current resolution*
  set *the centers of RBFs*
  set *the lookup table of the Wendland's RBF*
  for *each RBF center*
    approximate *the associated coefficients,* c_{xj}^l, c_{yj}^l, *and* c_{zj}^l *by minimizing Eq. (8)*
  end for
  accumulate *deformation field*
  if $l < L$ **than** $l = l+1$
end while

4. Results

The proposed method was compared with SPM2 [3], HAMMER [4], and ART [5]. The validation procedure can easily generate a lot of simulated image pairs with the spatial corresponding relations. The constructed images could emulate actual deformation of images.

4.1 Materials

The validations of registration methods need the known ground truth of the spatial mapping between images. Simulated deformation fields generated by selecting control points and applying landmark-based basis functions should be the simplest way. However, it is difficult to well model the spatial correspondence between brain structures.

The construction of simulated images and the comparisons of registration algorithms were divided into two stages. Firstly, the proposed method and SPM2 was compared using simulated images created by TPS transformation with selected landmarks. Secondly, SPM2 was applied to register numerous images and the generated deformation fields were used to compare our method with HAMMER and ART. This validation procedure could easily construct simulated images, and the obtained spatial mapping relation could describe realistic deformations of brain structures.

Four simulated T1-weighted MR images, SD-1~SD-4, were first constructed by TPS using sixteen pairs of control points in which eight pairs were used to fix image corners and others were placed in the region of interests. The sizes of the source image and the warped images were all 115×115×96 with voxel size 2 mm^3. Figure 3 shows that the differences between the source image and the constructed images were smooth and reasonable. In simulations, the images transformed by TPS and the original image were regarded as the reference images and the test image, respectively.

Figure 4 shows a simple diagram of the second stage, in which SPM2 was applied to register 58 T1-weighted MR images using the MNI-152 brain template as the target image. The size of the 58 MR images and the images warped by SPM2 were all 115×115×96 with voxel size 2 mm^3. In simulations, the 58 images warped by SPM2 and the obtained deformation fields were regarded as the target images and the ground truths, respectively, and the original images were used as the test images. Figure 5 demonstrates one pair of the simulated images.

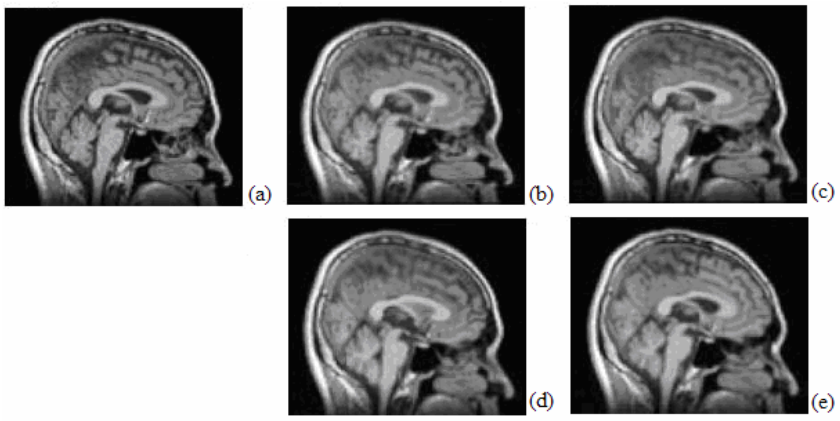

Figure 3. Simulated images constructed by TPS. The size of these images are all 115x115x96 with voxel size 2 mm^3. (a) The source image. (b)-(e) The images warped by TPS using 16 pairs of control points.

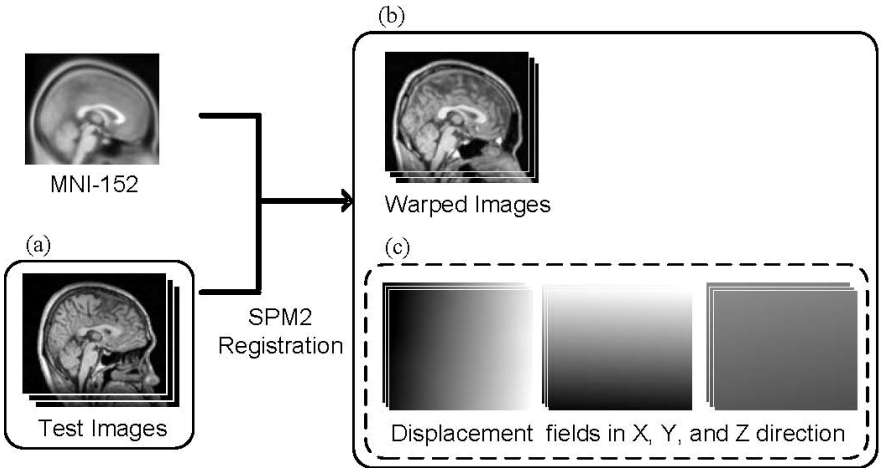

Figure 4. The construction of simulated images using SPM2. The MNI-152 brain template and 58 T1-weighted MR images were used to be the target image and the test images, respectively. In simulations, the 58 images registered by SPM2 (b), and the corresponding deformation fields (c), were regarded as the target images and the ground truths, respectively. The original images, (a), were used as the test images. The size of the original images and the registered images are all 115x115x96 with voxel size 2 mm^3.

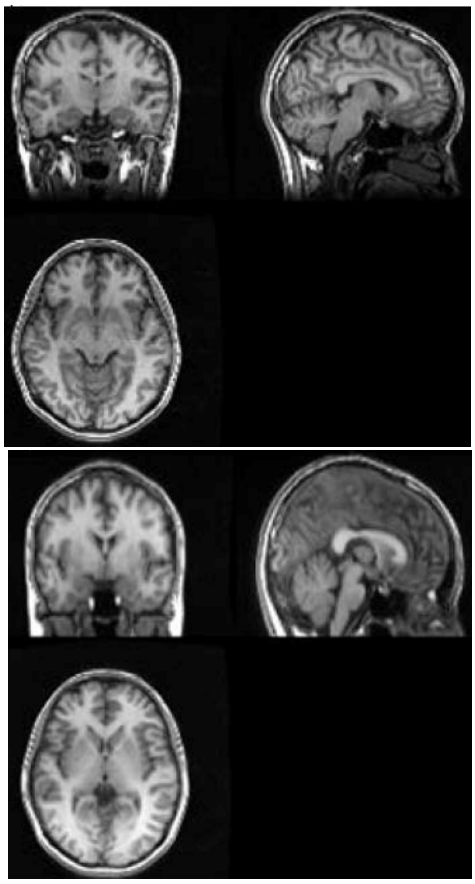

(a) (b)

Figure 5. One pair of the simulated images constructed by SPM2 using MNI-152 brain template as the target image. Image (b) is the registration result generated by SPM2 using image (a) as the test image.

4.2 Comparisons of registration algorithms

The default parameters of SPM2 were applied in the first simulation. The applied parameters of the proposed method were: 1) three levels of the image pyramid and the meshes of Wendland's RBFs; 2) the smoothing parameter α=0.5; 3) the parameter of the support length k=1.5; 4) the weighting of the approximated coefficients β=0.4; and 5) the parameter γ, set to be 0.6, which defined the area used to evaluate the registration cost. This work was implemented in C++ programming language, and the first simulation was performed on a PC with an AMD Athlon XP 2400+ processor running Windows-XP. Table 1 summarizes the simulation results, and it shows that our method is much more accurate than SPM2. The registration error in simulations of this work is defined as the average distance between the ground truth and the mapping location transformed by registration algorithms. Moreover, the error did not count the regions of non-brain tissues and the background.

Table 1. Accuracy comparisons with SPM2.

Method	Registration errors (mm)			
	SD-1	SD-2	SD-3	SD-4
SPM2 cutoff-25 mm (default)	1.65	1.60	1.58	1.61
SPM2 cutoff-20 mm	1.50	1.42	1.59	1.62
Our method	0.31	0.32	0.42	0.48

In the second simulation, the parameters of HAMMER and ART were set to be their defaults. The skull stripping and the tissue segmentation of each simulated image, which are two required preprocessing stages in HAMMER, were accomplished by the FSL package [26]. The parameters of the proposed method were the same as for the first simulation, except four mesh levels of RBFs were used instead. The simulation was executed on a PC with AMD Opteron 240 processor running Red Hat Linux. Table 2 shows the comparison results. These experimental results indicate that the proposed approach is superior to other methods in both accuracy and efficiency, except for the deviation variance was slightly larger than ART. The results indicate the accuracy of HAMMER is inferior to those of other methods. Table 3 summarizes the registration results of our method level by level, and it shows the increase of basis functions is useful to capture the local differences between structures.

Table 2. Accuracy and efficiency comparisons with HAMMER and ART.

Method	Registration errors	Variance	Time (sec)
HAMMER	1.70	0.76	2598
ART	0.69	0.09	522
Our method	0.48	0.13	309

Table 3. Registration errors and execution time of the proposed method at each level.

RBF number	23	43	83	163
Deviations (mm)	3.16	2.13	0.94	0.48
Variance (mm^2)	1.75	1.16	0.33	0.13
Time (sec)	<1	3	26	279

5. Discussion

An accurate and efficient nonlinear registration technique has been presented in this article. Hierarchical regular meshes of Wendland's RBFs are used to model coarse-to-fine deformation of images. Image registration is accomplished by a series of optimizations for the three coefficients associated with each mesh grid according to the spatial interpretation in deformation. This solves the difficulties of direct searching for coefficients in a huge optimization space. Our simulation results indicate the proposed method is much more accurate than SPM2 and is also superior to HAMMER and ART in both accuracy and efficiency.

The validation of registration techniques using real images is difficult because the spatial corresponding relations are always unknown. One method is to manually identify a set of corresponding landmarks between images by experts and quantify the deviation after registration. The major drawback of this approach is its requirement of manual selection of landmarks, and it also needs several experts to eliminate the subjective factor. Hence, this method is time-consuming and the landmark identification is always prone to errors.

Another frequently adopted validation method is to register several images to the same target. Registration techniques are evaluated according to the sharpness of the averaged results. The disadvantage is that the sharpness of an

average image may not a good criterion used to measure the accuracy of a registration technique. Firstly, one can always change the smoothing parameter to have a better result. Figures 6(a) and (b) demonstrate this by the average images of 57 T1-weighted MR volumes which were registered by SPM2 using different smoothing parameters, the maximum option and the default option. It can be seen that the default option resulted in a clearer image because the registrations were less regularized. In addition, Figure 6(c) shows the averaged image of the same 57 MR volumes which were registered by the proposed method. Though our averaged image is sharper than the two results of SPM2, it was penalized by larger deformation energy instead. Secondly, a clear average image could not imply that a registration technique is accurate. For example, ART was not robust in our experiments because the registration is quite less regularized and sensitive to noise. Image registration using ART is usually unstable (Figure 7(b)) and sometimes failed (Figure 7 (c)). However, the anatomical structures of the average image are quite clear, as shown in Figure 7 (a).

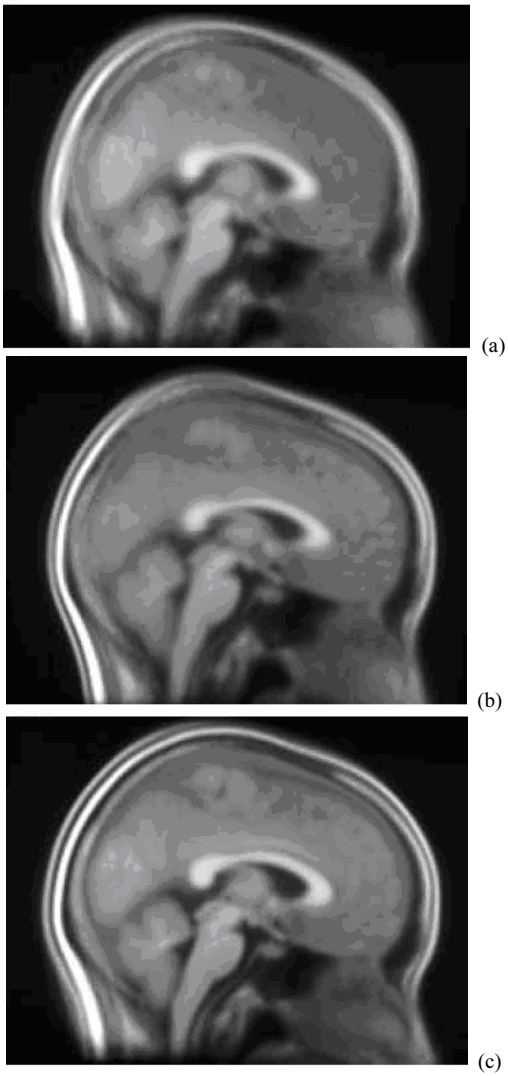

(a) (b) (c)

Figure 6. The averages of 57 T1-weighted MR images respectively registered by SPM2 using regularization parameter (a) 100, (b) 1, and (c) by the proposed registration method.

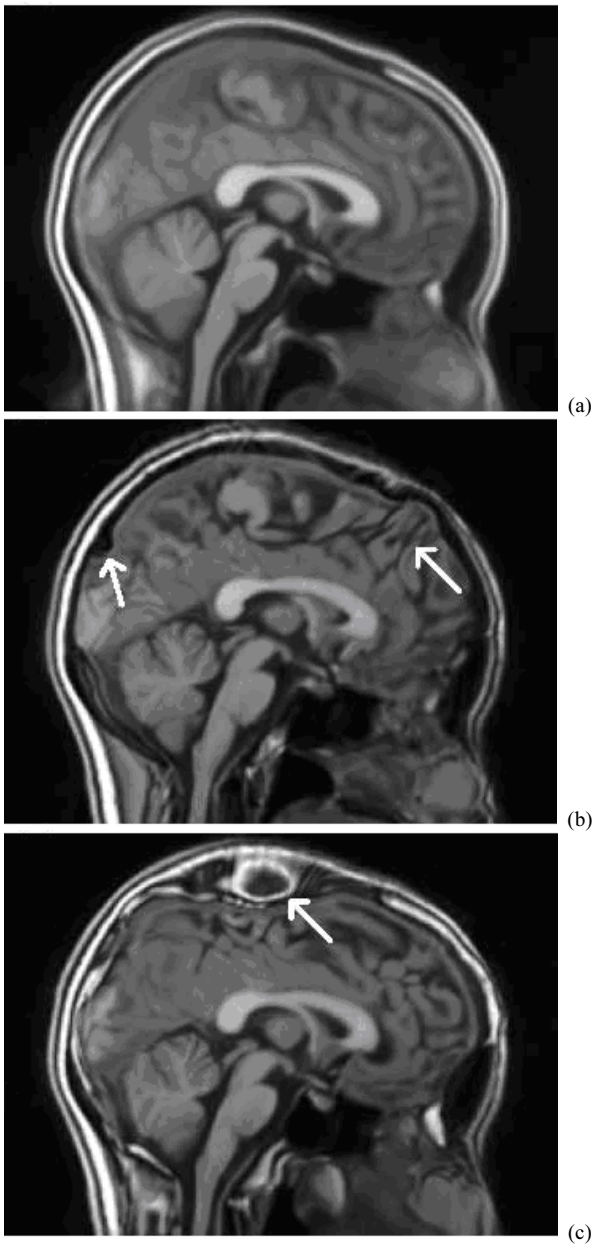

(a) (b) (c)

Figure 7. The performance of nonlinear registration algorithms should not be evaluated using the average of the aligned images. For example, the image averaged from the registration results of 57 real T1-weighted MR images using ART is quite sharp, as shown in (a). However, mostly registered images are less regularized, such as the regions indicated in (b), and the topology was not preserved in some registration results, such as the region indicated in (c).

Acknowledgements

This work was partially supported by National Science Council, Taiwan, under Grant NSC96-2752-B-075-001-PAE and Taipei Veterans General Hospital under Grant VGH V96ER1-003.

References

[1] R. P. Woods, S. T. Grafton, J. D. Watson, N. L. Sicotte and J. C. Mazziotta, "Automated image registration: II. Intersubject validation of linear and nonlinear models," *J. Comput. Assist. Tomogr.*, 22: 153-165, 1998.

[2] M. Fornefett, K. Rohr and H. S. Stiehl, "Radial basis functions with compact support for elastic registration of medical images," *Image Vis. Comput.*, 19: 87-96, 2001.

[3] J. Ashburner and K. J. Friston, "Nonlinear spatial normalization using basis functions," *Hum. Brain Mapp.*, 7: 254-266, 1999.

[4] D. Shen and C. Davatzikos, "HAMMER: hierarchical attribute matching mechanism for elastic registration," *IEEE Trans. Med. Imaging*, 21: 1421-1439, 2002.

[5] B. A. Ardekani, S. Guckemus, A. Bachman, M. J. Hoptman, M. Wojtaszek and J. Nierenberg, "Quantitative comparison of algorithms for inter-subject registration of 3D volumetric brain MRI scans," *J. Neurosci. Methods*, 142: 67-76, 2005.

[6] R. Bajcsy and S. Kovacic, "Multiresolution elastic matching," *Comput. Vision Graph. Image Process.*, 46: 1-21, 1989.

[7] H. Lester and S. R. Arridge, "A survey of hierarchical non-linear medical image registration," *Pattern Recognit.*, 32: 129-149, 1999.

[8] P. J. Edwards, D. L. G. Hill, J. A. Little and D. J. Hawkes, "Deformation for image guided interventions using a three component tissue model," *Inf. Process. Med. Imaging*, 1230: 218-231, 1997.

[9] M. Ferrant, A. Nabavi, B. Macq, F. A. Jolesz, R. Kikinis and S. K. Warfield, "Registration of 3-D intraoperative MR images of the brain using a finite-element biomechanical model," *IEEE Trans. Med. Imaging*, 20: 1384-1397, 2001.

[10] Y. Amit, "A nonlinear variational problem for image matching," *SIAM J. Sci. Comput.*, 15: 207-224, 1994.

[11] Y. T. Wu, T. Kanade, C. C. Li and J. Cohn, "Image registration using wavelet-based motion model," *Int. J. Comput. Vis.*, 38: 129-152, 2000.

[12] F. L. Bookstein, "Principal warps: thin-plate splines and the decomposition of deformations," *IEEE Trans. Pattern Anal. Mach. Intell.*, 11: 567-585, 1989.

[13] J. A. Little, D. L. G. Hill and D. J. Hawkes, "Deformations incorporating rigid structures," *Comput. Vis. Image Underst.*, 66: 223-232, 1997.

[14] N. Arad, N. Dyn, D. Reisfeld and Y. Yeshurun, "Image warping by radial basis functions-application to facial expressions," *CVGIP: Graph. Models Image Process.*, 56: 161-172, 1994.

[15] D. Ruprecht, R. Nagel and H. Muller, "Spatial free-form deformation with scattered data interpolation methods," *Comput. Graph.*, 19: 63-71, 1995.

[16] D. Rueckert, L. I. Sonoda, C. Hayes, D. L. Hill, M. O. Leach and D. J. Hawkes, "Nonrigid registration using free-form deformations: application to breast MR images," *IEEE Trans. Med. Imaging*, 18: 712-721, 1999.

[17] J. Kybic, P. Thevenaz, A. Nirkko and M. Unser, "Unwarping of unidirectionally distorted EPI images," *IEEE Trans. Med. Imaging*, 19: 80-93, 2000.

[18] B. Likar and F. Pernus, "A hierarchical approach to elastic registration based on mutual information," *Image Vis. Comput.*, 19: 33-44, 2001.

[19] G. K. Rohde, A. Aldroubi and B. M. Dawant, "The adaptive bases algorithm for intensity-based nonrigid image registration," *IEEE Trans. Med. Imaging*, 22: 1470-1479, 2003.

[20] B. Zitova and J. Flusser, "Image registration methods: a survey," *Image Vis. Comput.*, 21: 977-1000, 2003.

[21] J. P. Pluim, J. B. Maintz and M. A. Viergever, "Mutualinformation-based registration of medical images: a survey," *IEEE Trans. Med. Imaging*, 22: 986-1004, 2003.

[22] P. Viola and W. M. Wells, "Alignment by maximization of mutual information," *Int. J. Comput. Vis.*, 24: 137-154, 1997.

[23] A. Roche, G. Malandain, X. Pennec and N. Ayache, "The correlation ratio as a new similarity measure for multimodal image registration," *Proc. of the First Int. Conf. on Medical Image Computing and Computer-Assisted Intervention*,. 1496: 1115-1124, 1998.

[24] M. Jenkinson and S. Smith, "A global optimisation method for robust affine registration of brain images," *Med. Image Anal.*, 5: 143-156, 2001.

[25] J. P. W. Pluim, J. B. A. Maintz and M. A. Viergever, "Interpolation artefacts in mutual information-based image registration," *Comput. Vis. Image Underst.*, 77: 211-232, 2000.

[26] S. Smith, P. R. Bannister, C. Beckmann, M. Brady, S. Clare, D. Flitney, P. Hansen, M. Jenkinson, D. Leibovici, B. Ripley, M. Woolrich and Y. Zhang, "FSL: New tools for functional and structural brain image analysis," *Neuroimage*, 13: S249, 2001.